Remote Sensing of Environment 117 (2012) 281–288

Contents lists available at SciVerse ScienceDirect

Remote Sensing of Environment

journal homepage: www.elsevier.com/locate/rse

Assessing levee stability with geometric parameters derived from airborne LiDAR

A. Casas [a,*], D. Riaño [a,b], J. Greenberg [a,c], S. Ustin [a]

[a] Department of Land, Air, and Water Resources, University of California, Davis, CA 95616, USA
[b] Centro de Ciencias Humanas y Sociales, Consejo Superior de Investigaciones Científicas, Madrid, Spain
[c] Department of Geography, University of Illinois at Urbana-Champaign, Urbana, IL 61801, USA

ARTICLE INFO

Article history:
Received 6 April 2011
Received in revised form 29 September 2011
Accepted 4 October 2011
Available online 8 November 2011

Keywords:
LiDAR
Levee system
Topography
Stability
Flood risk
Geometry
Slope
Sacramento River

ABSTRACT

A methodology to assess levee structural integrity using high resolution airborne Light Detection and Ranging (LiDAR) data is investigated for a 16 km reach of the Sacramento River within the Sacramento–San Joaquin River Delta (California). Levee geometric parameters (levee crown width, height and water and landside slopes) were extracted from 0.5 m resolution LiDAR derived digital ground models. Deviation of these parameters from minimum levee design standards was used to calculate a levee stability index. Stability maps were generated and those areas that did not meet USACE geometric shape standards were identified. Results show that 2 out of the 4 geometric parameters do not meet the minimum value required in 48% and 43% of profiles on the east (urban adjacent) and west (farmland adjacent) margins respectively. Most importantly, the crown width in 99% of the levee profiles located on the urban side was below the minimum required. The paper also points out the importance of evaluating all four geometric parameters, not just the elevation of the levee, by assessing its level of performance through a geometric assessment.

1. Introduction

Floods have the greatest damage potential of all natural disasters worldwide affecting the greatest number of people (NISDR, 2002), and the risk of flooding is expected to rise due to climate change (sea level rise, higher intensity of storm events) and global change (changing land uses, proportion of flood vulnerable population), (Bates et al., 2008). Flood control infrastructures, such as levees, prevent high flows from entering flood prone areas, but no levee system reduces flood risk to zero (ASCE, 2010; Florsheim & Dettinger, 2007; Pinter, 2005). One third of the flood disasters in the U.S. have been related to levee failures (NRC, 1982) however homes and new infrastructure continue to be planned and built in flood-prone areas (Pinter, 2005) and levee-system maintenance though critical, is commonly underfunded (NCLS, 2009). The destructive consequences of erosion, inundation and sedimentation that involve a levee-failure flood, such as those occurred during Hurricane Katrina in 2005, constitute a high risk in other regions also protected by levee systems such as in the Sacramento–San Joaquin River Delta in California. Considering only the U.S., 43% of the nation's population live in counties protected by levees. California, along with Louisiana, Arkansas and Mississippi, is one of the States that rely most extensively on levees (ASCE, 2010).

The size and structure characteristic of any levee system, such as the minimum elevation, crown width or landside and waterside slopes, are usually defined by designed standards. In the US, minimum levee geometry criteria have been specified by various Corps and State guidance documents. The maintenance of a levee network over its lifetime is an important factor which will determine how optimally the levee will perform its protection role (ASCE, 2010). External forces, such as sea-level rise, subsidence, earthquakes or stream power, may act upon the levee over time provoking stress and eventually the failure of the levee (Dixon et al., 2006; Suddeth et al., 2010). Levee's structural failure may occur suddenly or progressively but in any case, prior to the failure, the initial geometric shape of the levee will be modified by producing slumping areas at the toe of the levee or sliding areas at the top of it. Levee degradation will modify its morphometry from the initial design standards, producing narrower crowns and/or lower levee side slopes. These external evidences of degradation in the levee geometry can be used to infer the degree of integrity and stability of a levee and a mean to assess the stability tipping points conducive to failure.

The geometry and stability of a levee is defined by profile and cross-section surveys or break-line topography. This information has been traditionally collected through transect-based topographic surveys in a precise and accurate but time and cost consuming way (Blake, 2010). Topographic surface-based data collection, such as airborne and terrestrial laser scanners (LiDAR) provide high resolution topography that have promoted the development of new research approaches in hydrology and geomorphology in the last years (French, 2003; Heritage & Hetherington, 2007; Lane & Chandler,

* Corresponding author. Tel.: +1 5302197687.
E-mail address: angelescasasp@gmail.com (A. Casas).

0034-4257/$ – see front matter © 2011 Elsevier Inc. All rights reserved.
doi:10.1016/j.rse.2011.10.003

2003). LiDAR data three dimensionality, high resolution and dense coverage over larger areas than those obtain with other technologies, such as GPS surveys, photogrammetry or terrestrial laser scanner (Ackerman, 1999), makes it particularly suitable as topographic source in numerical hydrodynamic modeling to increase the accuracy of flood hazard mapping (Casas et al., 2006; Marks & Bates, 2000; Mason et al., 2007), flood defense infrastructure assessment (Franken & Flos, 2005; Long et al., 2010), storm inundation analysis (Stoker et al., 2009), natural hazard management (Geist et al., 2009) and land surface processes in fluvial studies (Tarolli et al., 2009). LiDAR data has a great potential for the geometric assessment of the levee's degradation, although there is a lack of methodological proposals in the published literature.

In this paper, we present a method to assess the stability of a levee system and the identification of critical fragile sections through the characterization of the levee size and shape using LiDAR data. Geometric parameters relevant to the stability of the levee, such as crown width, elevation, and water and landside slopes are extracted and are compared with established minimum geometry design parameters (USACE, 2008). The deviation of these parameters measured from the minimum requirements provides an assessment of the condition of the levee. To achieve this, the first objective is to outline the levee dimension and extent and characterize it in terms of its geometric structural parameters and the second objective is to define a stability index of the levee based on the deviation of the actual geometry from design standards. Finally, the map with the stability condition of the levees will be used to investigate the relation between the location and the distribution of geometric degraded reaches.

2. Study area

The study reach site (Fig. 1) comprises a 16 km reach of the Sacramento River within the Sacramento–San Joaquin Delta Region (California, USA) characterized by a meandering river channel morphology, with point bar deposition areas. At this study reach, the Sacramento River borders a highly urbanized area on its east side in what it is called the Sacramento "pocket area" whereas the west margin borders agricultural lands. The channel banks, levees and nearby floodplain areas are covered by shrubs, herbaceous grasses, and mixed riparian forest (e.g. oak, walnut, cottonwood, and sycamore).

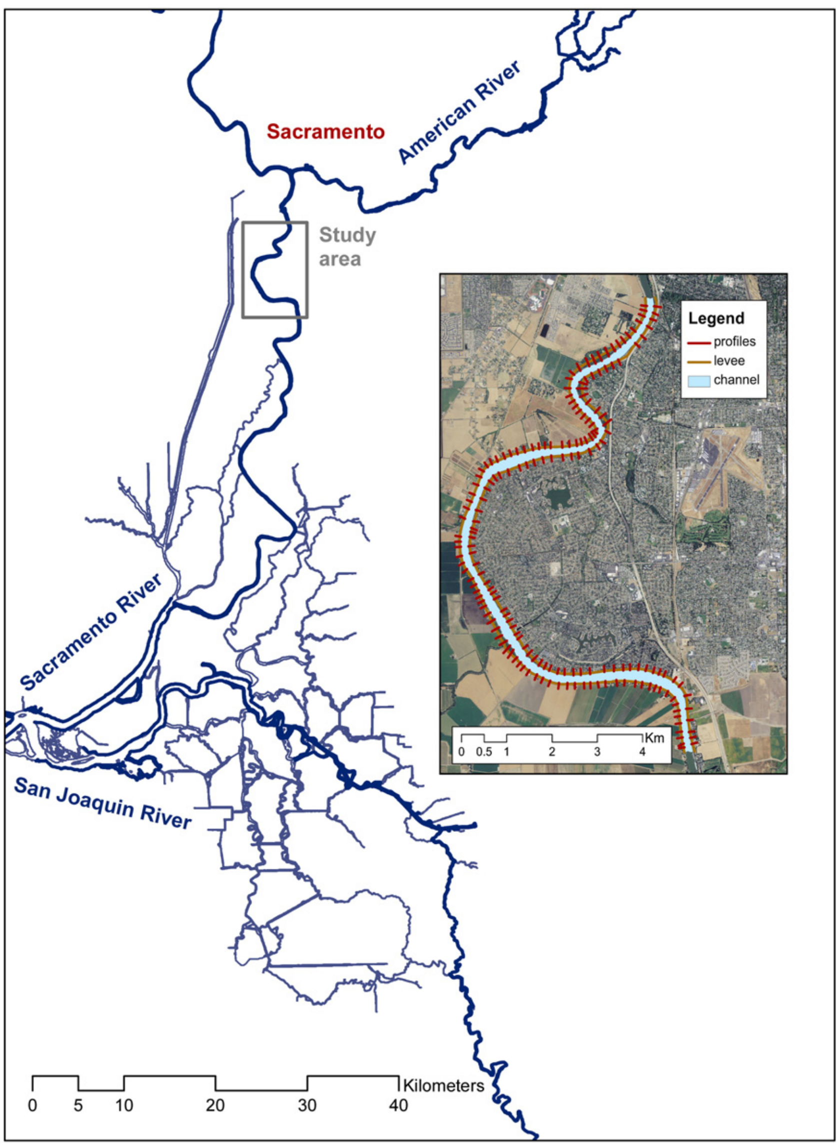

Fig. 1. Study reach location at the Sacramento River in the Sacramento–San Joaquin Delta Region in California. Including an orthophoto of the reach illustrating the LiDAR profiles location at the east and west margin of the river, the levees and the channel.

The Sacramento–San Joaquin Delta has approximately 2600 km of levees that protect urban and farmland, much of it below sea level, from flooding and erosion. Levees prevent saltwater intrusion into freshwater rivers which provides irrigation and much of the state's drinking water supply and control flood risk (Mount & Twiss, 2005; Suddeth et al., 2010). The city of Sacramento relies heavily on these levees to cope with flooding. Subsidence of peat soils, changing inflows, sea level rise and earthquakes are some of the processes that act upon the Delta levee network and produce continuous degradation that will lead, eventually, to the failure of the levees (Burton & Cutter, 2008; Moore & Schlemon, 2008). In the Delta, levees were constructed in different phases during the last 150 years, with many of them built of gravel, sand and silt, making them susceptible to erosion, seepage and breaches. Many levees were founded on unconsolidated, highly variable and permeable materials (USSD, 2009). Delta levees are particularly vulnerable to failure due to their location, aging, infrastructure, low elevation and subsidence. Currently, Sacramento–San Joaquin Delta levees are under an unprecedented evaluation to identify levee deficiencies and repair the critically damaged tracks, through the FloodSAFE California initiative (USSD, 2009). This evaluation has the goal of guarantee protection of urban areas for a flood with average recurrence interval of 200 years (0.5% exceedence probability) (DWR, 2010) for which field explorations, e.g. drilling, geophysical methods and laboratory testing, and geotechnical engineering analysis are programmed (USSD, 2009). According to the initiative, new flood maps are to be calculated taking into account the impact that climatic change may exert upon the size and the frequency of the floods, new regulations are in interim stages and LiDAR data has been acquired by the State of California, Department of Water Resources (DWR) for the entire Delta area.

3. Methodology

3.1. LiDAR data and surface derivations

The LiDAR data were supplied by the Department of Water Resources (DWR) and were originally acquired from a helicopter using an Optech ALTM-3100 flying at an average altitude of 1680 m (5500 ft) above ground level during the leaf-off conditions during late January and February of 2007. Data were delivered as first and last pulse data with an intended point density of 1 point/m^2. According to the vendor, the vertical accuracy is of $\pm$0.15–0.18 m and the horizontal accuracy of $\pm$0.3 m. The flying speed was 120 knots, the scan angle 12° and the pulse rate 70 kHz. The average swath width was of 711.44 m with an overlap of 40%. The vendor provided a classified data set of points as bare earth extracted from the last pulse return.

A Digital Ground Model (DGM) was generated with the classified bare earth LiDAR dataset using natural neighbor (Sibson, 1981) interpolation at 0.5 m resolution. Resolution has a significant impact upon surface slope and surface derivatives (Oksanen & Sarjakoski, 2005). There is no precise rule about the grid resolution of a model as a function of the spacing or density of measured data but ideally the pixel size is selected to provide at least a measured point to each cell of the grid. However, the irregular distribution of LiDAR clouds makes this selection difficult. A resolution of 0.5 m, which is the finest spacing found between LiDAR data points, was chosen as pixel size for the topographic model to encompass all the spatial variability collected at the measurement scale of the data. A 1 m-DGM was generated and the comparison between LiDAR ground points with the 0.5 m-DGM and 1 m-DGM interpolated using Natural Neighbor was calculated and results in RMSE values of 0.0413 m and 0.071 m, respectively. Finer mesh resolution than the nominal post spacing are found in literature in geomorphological (e.g. Pirotti & Tarolli, 2010) and forest structure (e.g. Bater et al., 2007; Falkowski et al., 2006) applications.

The natural neighbor method was chosen to interpolate the data given the irregular distribution of the LiDAR data and the requirement of the interpolated model to preserve as much topographic content and variability as possible in a gridded mesh, which is needed to outline the shape of the levee and its morphology. Natural neighbor interpolators, together with linear interpolators, tend to have the lowest overall range of errors when compared with measured data (Bater & Coops, 2009). This method has been chosen recently in several studies related to the use of LiDAR data for extracting geomorphic features such as channel network (Pirotti & Tarolli, 2010) and landslide crowns and bank erosion (Tarolli et al., 2010), analysis of debris flow events (Scheidl et al., 2008), forest structure (Bater et al., 2007; Falkowski et al., 2006; Goodwin et al., 2006) and topography for flood inundation modeling (e.g. Liang et al., 2008). Natural neighbor interpolation is based on an initial layer of Voronoi polygons created with measured data. A new Voronoi tessellation is created with the points to be interpolated, the final value is assigned to the grid cell according to weights calculated using the area ratio between overlapped Voronoi polygons at that location (Sambridge et al., 1995; Sibson, 1981).

A slope model was derived from the DGM, as a geometrical property of the land surface. The slope was calculated adopting the method of taking the first derivative of a bi-quadratic polynomial representing a local extent of a surface (e.g. Evans, 1990). The standard method to solve the polynomial expression is to calculate the parameters of a central cell in relation to its eight neighbors, passing a 3×3 local window over the gridded surface. A function of the first derivative has been used, (gradient), since functions of higher order DGM derivatives (such as curvatures) are more sensitive to DGM noise (Zhou & Liu, 2004) complicating the definition of the levee geometry. In relation to the elevations in a DGM, the gradient is a vector pointing in the direction of the maximum variation. The slope is the length of the gradient and reflects the maximal rate of change of elevation values and the aspect corresponds with the slope direction. Both are useful to recognize the inclined shape and the flat crown of the levee. Several methods for slope calculation have been reported in literature. In this paper, the average maximum technique was used, where the maximum slope in the vertical and horizontal directions averaged (Srinivasan & Engel, 1991).

3.2. Levee delineation and geometry

The typical shape of a levee section (Fig. 2) has two inclined areas, with a water body on one side and dry land on the other, between these, an elevated central flat area defines the levee crown. The limit between the inclined areas and the crown is defined by two hinge points, with a break in the slope, which demarcates the levee crown from the inclined sides. In this research, the main parameters extracted to define the levee geometry are: elevation, crown width, and the slopes in the waterside and in the landside in accordance

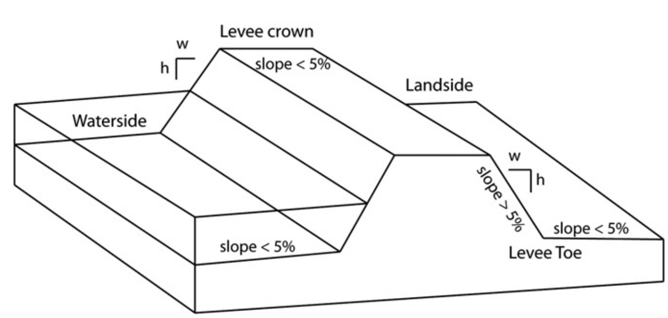

Fig. 2. Sketch of the geometry levee definition.

Table 1
Descriptive statistics of levee parameters.

	Levee height (m)		Crown width (m)		Slope waterside (%)		Slope landside (%)	
	E margin	W margin	E margin	W margin	E margin	W margin	E margin	W margin
Minimum	9.7	9.8	0.9	1.0	23	27	6	13
Maximum	13.6	13.0	10.5	15.4	56	53	47	51
Mean	11.0	11.3	3.3	5.5	39	41	34	33
Median	10.5	11.4	3.2	5.4	41	41	36	34
Standard deviation	0.9	1.0	1.2	2.6	7	6	8	6

with the geometric criteria specified in levee design guidance documents (e.g. USACE, 2000).

Topographic levee profiles have been delineated perpendicular to the river margin at 185 locations at ~150 m interval along the study site on both margins (Fig. 1). These profiles show a large variability in morphometry which increase the difficulty of a precise definition of the geometric parameters since levees form a continuum with the floodplain terrain and the crown delineation from the inclined areas are not sharply defined. Levee topographic transects were examined and variation in slope analysis showed that transition from levee crown surface to inclined sides occurred at a 5% slope. This criterion was also used to demarcate the inflection point between the levee itself (slope > 5%) and the floodplain land, at the levee toe in which the terrain becomes virtually flat over a short distance (Fig. 2).

The levee feature is classified from the DGM using the 5% slope criteria in the slope model within a buffered area of 150 m by the river margins. The crown is identified as the area within the levee with a slope below 5%. Once the levee extension and its crown are defined in the DGM, geometric parameters can be extracted from the profiles. The crown width can then be measured as the transect distance across the top of the levee profile with a slope below 5%. The elevation of the levee is the mean value of the points in the profile within the crown levee. The slopes were calculated as the ratio between the height and width of the sloped area. The levee toe in the landside and waterside were defined using the 5% criteria. The slopes were calculated as the gradient of the line fitted from the hinge point that separate the crown from the inclined area at the top of the levee and levee toe in the region adjacent to the water and in the landside.

3.3. Vulnerability to failure map

A levee stability index was developed comparing the current geometric parameters at each levee transect with the design standards. The stability index results from the addition of number of parameters out of the four calculated that do not meet the minimum geometry. This index defines the level of instability in terms of its current shape conditions and identifies those levee transects with higher failure vulnerability which can be represented as a vulnerability to failure map (Fig. 4). Minimum levee geometry criteria have been specified by various U.S. Corps of Engineers and California State guidance documents. In addition, the legislation and levee design criteria is under current development (DRW, 2010) for the study area. In this paper, the geometric minimums were established considering the most recent design guidance in the region for urban and urbanizing areas (USACE, 2008). According to these standards, the levee requires a minimum crown width of 20 ft (6.09 m), minimum waterside levee slope with a ratio of 3 h:1 v (41%) and a minimum landside levee slope of 3 h:1 v for new levees and 2 h:1v (60%) for existing levees with good performance. The minimum levee elevation is estimated to reach in excess of 3 ft (0.9 m) the water surface elevation for a peak discharge with average return interval of 200 years (0.5% annual probability flood).

4. Results

Table 1 summarizes the statistics of the parameters for each profile according to those along the east or west margin of the river. The east margin (urban) presents lower mean and median elevation values. The mean and median waterside slope is also lower in the east (urban) margin whereas the lower slope values are found in the landside of the west margin, i.e. towards the landside on the non-urban river margin. It must be also pointed out the 2 m of difference in the mean and median crown width between the east and the west margins, where the narrowest corresponds to the east margin, adjacent to the urban area.

Levee geometry results are presented in terms of the percentage of profiles within a specified range of values for each parameter, for locations on each side of the river (Tables 2 and 3). Table 2 shows how the most frequent crown width in the urban margin (73% of profiles) falls between 2 and 4 m, whereas the most frequent range in the west margin (34% of profiles) falls within a wider crown interval (4 to 6 m). In terms of elevation, in the urban margin 49% of profiles are less than 10.5 m and about 70% below 11 m, whereas in the west margin, only 44% of profiles are less than 11 m. It is clear from Table 3 that most profiles have slopes between 30 and 50% along both margins. Slopes on the waterside have higher percentages between 40 and 50%, whereas on the landside the higher percentages correspond to lower slopes, with a 52% of profiles on the east margin and 71% on the west, between 30 and 40%.

Comparing the extracted parameters with the levee geometry criteria specified in the Geotechnical Levee Practice (USACE, 2008) allow classification of the levees in terms of good or poor condition for the considered geometric parameter (see Table 4). Fig. 3 plots each parameter and its condition along the studied reach. Ninety-nine percent of profiles on the east (urban) margin of the river do not meet the minimum crown width criteria. On the west margin, 62% are below the minimum criteria. Fig. 3 shows that the location of levees that meet the crown width condition on the west margin are distributed mainly in the southern part of the wider bend that contains the pocket area levees within the study reach. In terms of the levee elevation, it was assumed that all the levees are above the designed hydraulic top of the levee according to the IDLC (DWR, 2010). Note that the levee height criterion is not represented in Fig. 3 since all

Table 2
Percentage of profiles at different ranges of parameters – crown width and elevation – divided by its margin location.

Crown width (m)	% profiles		Elevation (m)	% profiles	
E margin	W margin	E margin	W margin	E margin	W margin
0–2	11	7	<10	5	9
2–4	73	22	10–10.5	44	27
4–6	15	34	10.5–11	20	9
6–8	0	26	11–11.5	6	7
8–10	0	7	11.5–12	7	9
10–12	1	3	12–12.5	7	27
12–14	0	1	12.5–13	7	11
14–16	0	1	>13	4	2

Table 3
Percentage of profiles at different ranges of parameters – waterside and landside slopes – divided by its margin location.

Slope (%)	% of profiles (waterside)		% of profiles (landside)	
Ranges	E margin	W margin	E margin	W margin
<20	0	0	5	3
20–30	8	6	17	22
30–40	37	37	52	71
40–50	52	50	26	3
50–60	2	8	0	1

profiles are above the minimum. An initial value of the 200-year water surface elevation (29.03 ft, MBK, 2008) was used to assess the levee elevation parameter, considering the lowest point of the reach (Freeport station). The minimum elevation of the levee should be this value plus the freeboard, which is 9.8 m. According to this value, all the levees of the reach meet the minimum hydraulic top of the levee criteria. In terms of the waterside slopes, about half of the levees on the west and the east margin are below the minimum criteria, whereas on the landside, 80% and 98% do not meet the minimum slope on the east (urban) and west margins, respectively.

Table 5 presents the percentage of transects in relation to the number of parameters out of the four measured that are below the minimum levee stability criteria. Therefore those that fail in one out of four parameters are in a better condition (Good) than those with three parameters below the criterion minima (Poor). The table shows that on the east (urban) margin 42% of profiles fail on three out of four parameters and 48% do not meet two of them (Fair), whereas in the west margin, 33% fail on three out of four criteria and 43% on two of the four criteria. Fig. 4 represents the spatial distribution of these results along the river reach.

5. Discussion

The maintenance of the integrity of the levees in Sacramento–San Joaquin Delta system constitutes a continuous challenge, due to its tidal estuary nature, tectonically unstable location, and climate change impacts upon sea level rise and flood occurrence (Coleman, 1988; USSD, 2009; Weiss et al., 2011). California relies heavily on the Sacramento San Joaquin Delta levees for water supply, water quality, land use, agricultural purposes and protection of flood vulnerable urban and urbanizing areas. An automatic method to assess periodically the stage of levee degradation over large regions may facilitate the early detection of weakened levee sections and the later decision for maintenance and repairing works. The benefits of using LiDAR as a topographic source in flood inundation modeling (e.g. Bates et al., 2003) has promoted its acquisition in recent years in lowland areas with high risk of flooding, such as the Sacramento–San Joaquin Delta. This cartographic source also offers a new potential for levee characterization as a superficial feature in the landscape.

In this paper, we present a method to assess the integrity of levees in terms of its structural geometry using LiDAR data. The paper demonstrates how the geometry of the levee can be obtained and used to establish a stability index. The most relevant parameters for the stability of the levee were selected and extracted for each profile considered. Based on the geometric criteria considered in most levee design documents, the parameters selected were: elevation, crown width and slopes on both water and landside. The elevation of the levee determines the maximum stage of the water in which the levee will be not overtopped and is the main parameter traditionally considered to assign a level of protection to a levee reach (DWR, 2010). It must be pointed out that most of the lands in the Delta are below sea level therefore these levees act as dikes, continuously holding back the in-channel water. It is also noteworthy that the last major levee-failure flood took place in Upper Jones Track in 2004 and the specific reason, although unknown, was not flow overtopping. The full geometric parameterization of the levee (elevation, crown width and slope) can be used to identify stressed levees which may collapse before overtopping occurs. A low slope together with a narrow crown may be produced by internal or external erosion which might be an indicator of the poor condition of the levee and evidence a higher risk of failure, even if the narrow crown meets the minimum elevation criteria. Fig. 3 shows areas where three of four shape parameters do not meet the USACE standards in a highly populated area. In the urban margin (E), results show that the mean value of the crown width parameter is of 3.3 m (Table 1) and 99% of the levees are narrower than the minimum required (Table 4). This condition and the fact that 81% of the profiles in the landside with slopes less than minimum required (41%) might imply an important degradation of the levees, even if the minimum elevation of the levee criteria is reached for the area. From the west margin, it should also be noted that 98% of the profiles have a landside slope below the minimum, though levee elevations are higher than those in the east margin.

The extraction of the parameters relies on the way the levee is outline from the continuum of the terrain and of the LiDAR data. To delimitate the levee slope, a criteria of 5% slope for flat areas was chosen. The 5% slope threshold was selected after evaluating the topography of the levees within the reach. Once levees were demarcated using a derivative approach to the DGM, the crown area within the fore and back slopes was demarcated, again using the 5% slope criteria, assuming the crown is flat up to the start of a slope, defined as a 5%. To define the slopes, the selected method consists of the gradient of the line which was fit from the hinge point in the crown to the toe of the levee. Other criteria were considered such as the median slope values obtained in the profile, this method would be interesting, given that it captures information about the roughness of the terrain in the profile, but we selected a traditional engineering surveying method to compare the slope values against the design standards.

The impact of the DGM resolution upon the parameters was also considered and parameters were calculated for 1 m-DGM and compared with 0.5 m-DGM results. The normalized percentage of the difference between the 1 m results and the 0.5 m results, showed a mean difference (0.5–1.0 m) of 0%, −31%, −10% and −10% for the levee height, crown width, slope landside and slope waterside, respectively for the east margin (urban side) and 0%, −20%, −4% and −1% for the west margin (agricultural side). As expected for the 1 m case, the width of the crown is wider and slopes are steeper due to the averaging of topography and displacement of the break in slope due to the cell size. The 1 m case reduces the number of profiles that do not meet USACE specifications and this could underestimate an assessment of the risk of levee failure.

Table 4
Percentage of profiles that meet minimum levee geometry criteria (Good) in terms of crown width, waterside slope, and landside slope according to USACE (2008).

	Levee height	% profiles		Slope landside	% profiles		Slope landside	% profiles		Slope waterside	% profiles	
Condition	Range (m)	E margin	W margin	Range (%)	E margin	W margin	Range (%)	E margin	W margin	Range (%)	E margin	W margin
Good	≥9.8	100	100	≥6.1	1	38	≥41	19	2	≥41	49	53
Poor	<9.8	0	0	<6.1	99	62	<41	81	98	<41	51	48

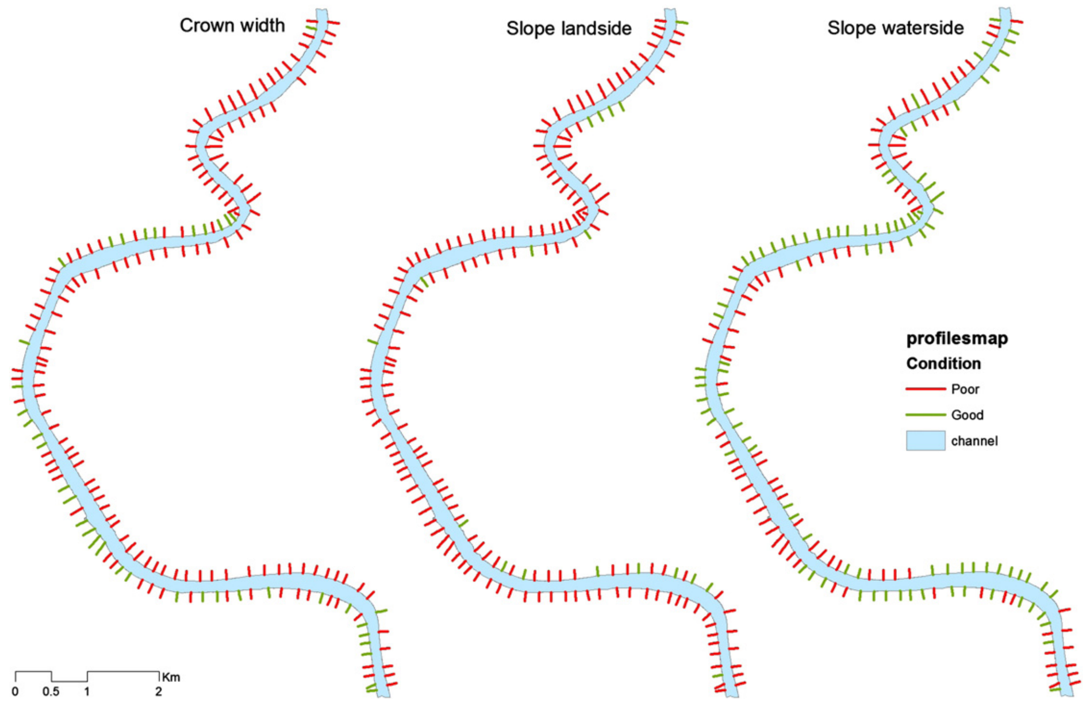

Fig. 3. Geometric parameters map. Condition stability ranges for crown width (m): good (≥6.1), poor (<6.1); landside slope and waterside slope (%): good (≥41), poor (≤41), according to USACE (2008).

Comparison of the parameters with design standards presented a difficulty due to the lack of specific guidance from the federal government on levee design considerations. Furthermore, there are no procedural criteria that would be applicable in making a finding that the urban level of flood protection exits for an area (DWR, 2010). Floodplain development projects in Sacramento–San Joaquin Delta are constrained by FEMA guidelines and administered by the Corps of Engineers. The Sacramento–San Joaquin Valley regulation is currently using interim analytical and procedural criteria to follow in meeting the requirements to find that levees and floodwalls provide protection against a flood with an annual average recurrence interval of 200 years (0.5% occurrence probability). In this paper, the most recent one of those considered in the interim criteria was selected (USACE, 2008).

The stability index, obtained in this paper, has been compared with the flood zone designations according to the level of flood risk provided by the FEMA where each zone reflects the severity or type of flooding in the area. According to FEMA, levees on the east margin are within a zone designated as high risk with a 1% annual probability of being exceeded whereas the levees on the west margin are within a zone of moderate risk defined by the 500 years recurrence interval (0.2% probability flood). This implies that the levees on east (urban)

Table 5
Percentage of transect at different stability conditions at the east and west margins. The condition fraction means that the parameters below the minimum geometry criteria (USACE, 2008) out of the four parameters considered (width, height, waterside slope, and landside slope).

	% profiles	
Condition	E margin	W margin
Very Good – 0/4	0	0
Good – 1/4	11	25
Fair – 2/4	48	43
Poor – 3/4	42	33
Very Poor – 4/4	0	0

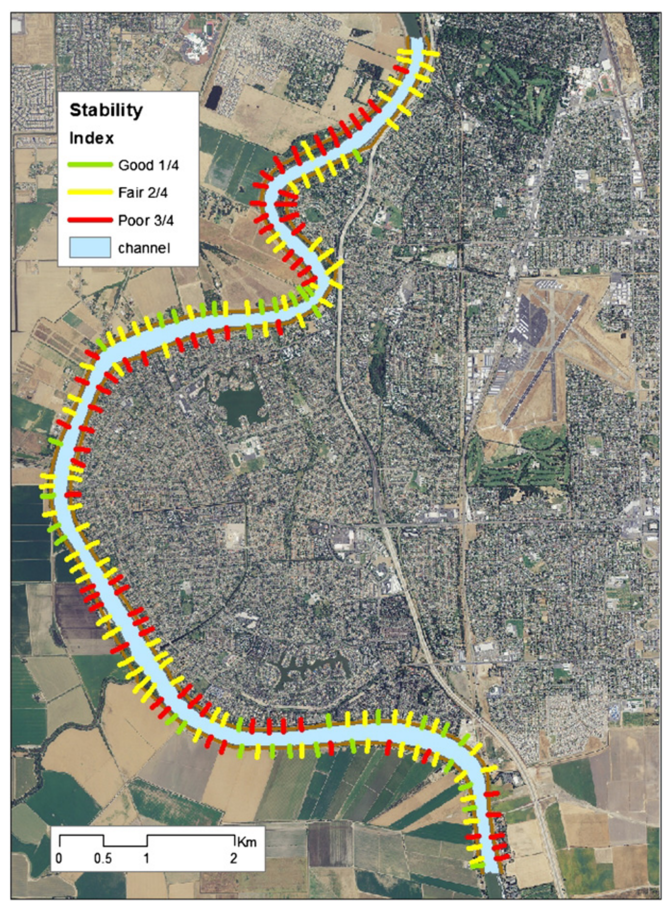

Fig. 4. Stability map according to the risk of failure of each levee in terms of its geometry. A stability condition (good, fair or poor) is assigned to each levee depending on the geometric parameters (width, elevation, waterside slope and landside slope) that do not meet design standards, according to USACE, (2008).

margin will protect the urban area up to a 100 year return period flood. These flood risk zones agree with the results in this paper (Table 5) given the higher percentage of levee transects in worse conditions in the east margin than in the west one. However, in the FEMA approach, overtopping is considered the primary cause of levee failure meaning that levee performance and stability is assessed based on levee height associated to a flood stage with a return period of 200 years. This paper shows that levee elevation on the urban side is lower than on the west farm land margin. Moreover, this study also points out that 42% of the levee transects on the east side (Table 5) shows degradation problems and therefore a potential stability risk of failure in case of occurrence of a 1% annual probability flood. At the same time, the levee design for a 100-year flood protection on the east margin may be misleading, given the poor condition of the geometry of the levees (see Table 5), which may contribute to a collapse of the levee prior overtopping (e.g. seepage erosion). It must be noted that floodplain maps throughout the nation are being updated by FEMA under its Map Modernization Program and in its new approach, overtopping is not the only cause of failure to be considered and more weight is planned to be given to slope instability and erosion stage (Department of Water Resources, DWR., 2010). Our results are relevant, given the developing stage of the Central Valley Flood Management Planning Program (FloodSAFE) and the availability of high resolution LiDAR data. LiDAR are shown to be useful not only to improve hydrodynamic modeling processes and therefore flood inundation maps, but to characterize flood defense infrastructures such as levees, assess their morphometry and identify weakened tracks.

This paper states the importance of LiDAR as the cartographic source to extract well known geometric parameters relevant in levee design and maintenance and an assessment of the levee not only in terms of its elevation, but of its shape and size. We present a new approach to assess the geometry of the levees using LiDAR data to characterize and assess their integrity. LiDAR is used in flood hazard assessment to provide a fast and automatic evaluation of the geometric condition of the levees once the parameter definition and the threshold are defined. An initial index of the stability condition of the levees was inferred and the tracks with a higher risk of failure where maintenance operation should be a priority, identified. Thus, LiDAR can provide an initial automated assessment of the stability condition to support specific geotechnical explorations, which requires extensive fieldwork, including drilling and geophysical methods, along with associated laboratory testing and modeling procedures, such as seepage modeling, hydraulic modeling, slope stability, or fragility analysis (URS Corporation, J. R. Benjamin & Associates, 2009). Such methods could be applied once a potential hazard has been identified, thus providing more efficient use of management resources.

6. Conclusions

This paper describes a method to assess the stability condition of levees using LiDAR data. The approach is based on the geometric characterization of the levee feature and the extraction of it most relevant parameters, namely crown width, elevation, waterside and landside slopes. The comparison of these parameters with minimum designed standards provides an index of the integrity condition of the levee. This geometric index is used to identify geometrically weakened levee reaches and therefore those with a higher risk of failure and with an urgency to be repaired. Results show that a comprehensive understanding of the integrity condition of the levee requires use of the four geometric parameters, not just elevation, given the impact that degrading processes have on parameters such as crown width or slope. LiDAR provides an effective way to assess the external geometry of the levees to detect areas prone to failure as those that deviate from the required geometry. Levee characterization results show that the east river margin, which corresponds to the levee that protects the urban side, has narrower crowns and lower waterside slopes. The levee elevation along the urban margin is also lower, with 70% of profiles below 11 m, whereas 44% of profiles on the west margin are below 11 m. The comparison of geometric parameters with levee design criteria shows that 99% of profiles in the urban margin failed to meet the USACE minimum crown width criteria. The levees on the west margin are 62% below the minimum width. In terms of the waterside slopes, about half levees on the west and the east margins are below the minimum criteria, whereas on the landside 81% and 98% do not meet the minimum on the east (urban) and west margins respectively. Finally, 42% of profiles on the east (urban) margin do not meet three out of four minimum geometric criteria and 48% failed on two of them, whereas on the west margin (farm land), 33% failed on three out of four and 43% on two of the four criteria.

Acknowledgments

Ángeles Casas was supported by a postdoctoral grant of the Spanish Ministry of Education and Science. The authors thank the California DWR (Department of Water Resources) for the provision of the LiDAR data used in this study and funding, entitled 'Analysis of the Integrity of the Levee System in the Sacramento Delta' from UC Santa Cruz under a grant under the University-Ames Research Consortium (UARC). The authors also thank Mui Lai and the Center for Spatial Technologies and Remote Sensing (CSTARS), University of California Davis for computer resources. We would like to thank Dr. Gerardo Benito for his insightful comments.

References

Ackerman, F. (1999). Airborne laser altimetry — Present status and future expectations. *ISPRS Journal of Photogrammetry and Remote Sensing*, *54*, 64–67.

American Society of Civil engineers (ASCE) (2010). *So, you live behind a levee.*

Bater, C. W., Coops, N. C., Gergel, S. E., & Goodwin, N. R. (2007). Towards the estimation of tree structural class in Northwest coastal forests using LiDAR sensing. *ISPRS Workshop on Laser Scanning 2007 and silviLaser 2007*. Finland: Espoo.

Bater, C. W., & Coops, N. C. (2009). Evaluating error associated with LiDAR-derived DEM interpolation. *Computers and Geosciences*, *35*(2), 289–300. doi:10.1016/j.cageo.2008.09.001.

Climate change and water. Bates, B. C., Kundzewicz, Z. W., Wu, S., & Palutikof, J. P. (Eds.). (2008). *Technical Paper of the Intergovernmental Panel on Climate Change*. Geneva: IPCC Secretariat 210 pp..

Bates, P. D., Marks, K. J., & Brasington, J. (2003). Optimal use of high-resolution topographic data in flood inundation models. *Hydrological Processes*, *17*, 537–557.

Blake, L. (2010). Levee networks in low-lying coastal areas. *ACSM Bulletin*, *246*, 10–16.

Burton, C., & Cutter, S. L. (2008). Levee failure and social vulnerability in the Sacramento–San Joaquin Delta area. *Natural Hazards Review, ASCE*. doi:10.1061/(ASCE)1527-6988(2008) 9:3(136).

Casas, A., Benito, G., Thorndycraft, V. R., & Rico, M. (2006). The topographic data source of digital terrain models as a key element in the accuracy of hydraulic flood modelling. *Earth Surface Processes and Landforms*, *31*, 444–456.

Coleman, J. M. (1988). Dynamic changes and processes in the Mississippi River delta. *Geological Society of American Bulletin*, *100*, 999–1015. doi:10.1130/0016-7606(1988)100<0999:DCAPIT>2.3.CO;2.

Department of Water Resources (DWR). (2010). *Interim levee design criteria for urban and urbanizing areas in the Sacramento–San Joaquin Valley*. : FloodSAFE Program.

Dixon, T. H., Amelung, F., Ferretti, A., Novali, F., Rocca, F., Dokka, R., Sella, G., Kim, S. -W., Wdowinski, S., & Whitman, D. (2006). Space geodesy: Subsidence and flooding in New Orleans. *Nature*, *441*, 587–588 (http://dx.doi.org/10.1038/441587a).

Evans, I. S. (1990). General geomorphometry (2.3). In A. S. Goudie (Ed.), *Geomorphological techniques* (pp. 44–56). (2nd edition). London: Unwin Hyman.

Falkowski, M. J., Smith, A. M. S., Hudak, A. T., Gessler, P. E., Vierling, L. A., & Crookston, N. L. (2006). Automated estimation of individual conifer tree height and crown diameter via two-dimensional spatial wavelet analysis of LiDAR data. *Canadian Journal of Remote Sensing*, *32*(2), 153–161.

Florsheim, J. L., & Dettinger, M. D. (2007). Climate and floods still govern California levee breaks. *Geophysical Research Letters*, *34*, L22403. doi:10.1029/2007GL031702.

Franken, P., & Flos, S. (2005). Using a helicopter based laser altimetry system (FLI-MAP) to carry out effective dike maintenance and construction policy. In van Beek, & Taal (Eds.), *Floods, from defense to managements – Van alphen*. London: Taylor & Francis Group ISBN 0 415 38050 2.

French, J. R. (2003). Airborne LiDAR in support of gemorphological and hydraulic modelling. *Earth Surface Processes and Landforms*, *28*, 321–335.

Geist, T., Hofle, B., Rutzinger, M., Pfeifer, N., & Stotter, J. (2009). Laser scanning — a paradigm change in topographic data acquisition for natural hazard management in

Sustainable Natural Hazard Management in Alpine Environments. In E. Veulliet (Ed.), : Springer-Verlag Berlin Heidelberg.

Goodwin, N. R., Coops, N. C., & Culvenor, D. S. (2006). Assessment of forest structure with airborne LiDAR and the effects of platform altitude. *Remote Sensing of Environment*, *103*(2), 140–152. doi:10.1016/j.rse.2006.03.003.

Heritage, G. L., & Hetherington, D. (2007). Towards a protocol for laser scanning in fluvial geomorphology. *Earth Surface Processes and Landforms*, *32*, 66–74.

Lane, S. N., & Chandler, J. H. (2003). Editorial: the generation of high quality topographic data for hydrology and geomorphology: New data sources, new applications and new problems. *Earth Surface Processes and Landforms*, *28*, 229–230.

Liang, Q., Du, G., Hall, J. W., & Borthwick, A. G. L. (2008). Flood inundation modelling with an adaptive quadtree grid shallow water equation solver. *ASCE, American Society of Civil Engineers*, *134*, 11. doi:10.1061/(ASCE)0733-9429(2008) 134:11(1603).

Long, G., Mawdesley, M. J., Smith, M., & Taha, A. (2010). Simulation of airborne LiDAR for the assessment of its role in infrastructure asset monitoring. In W. Tizani (Ed.), *Proceedings of the international Conference on computing in civil and building engenerering*. Nottingham University Press.

Marks, K. J., & Bates, P. D. (2000). Integration of high resolution topographic data with floodplain flow models. *Hydrological Processes*, *14*, 2000–2109.

Mason, D. C., Horritt, M. S., Hunter, N. M., & Bates, P. D. (2007). Use of fuse airborne scanning laser altimetry and digital map data for urban flood modelling. *Hydrological Processes*, *21*, 1436–1447.

Moore, J., & Schlemon, R. (2008). Levee system fragility. In M. C. Healy, M. D. Dettinger, & R. B. Norgaard (Eds.), *The state of Bay-Delta Science*. Sacramento, CA: CALFED Science Program.

Mount, J., & Twiss, R. (2005). Subsidence, sea-level rise, and seismicity in the Sacramento–San Joaquin Delta. *San Francisco Estuary and Watershed Science*, *3*(1) Article 5. http://repositories.cdlib.org/jmie/sfews/vol3/iss1/art5.

National Committee on Levee Safety. (2009). *Recommendations for a National Levee Safety Program*. .

National Research Council (NRC) (1982). *Levee policy for the National Flood Insurance Program*. Washington DC: National Academy Press.

Oksanen, J., & Sarjakoski, T. (2005). Error propagation of DEM-based surface derivatives. *Computers and Geosciences*, *31*(8), 1015–1027.

Pinter, N. (2005). One step forward, two steps back on U.S. floodplains. *Science*, *308*, 207–208.

Pirotti, F., & Tarolli, P. (2010). Suitability of LiDAR point density and derived landform curvature maps for channel network extraction. *Hydrological Processes*, *24*, 1187–1197. doi:10.1002/hyp. 7582.

Sambridge, M., Braun, J., & McQueen, H. (1995). Geophysical parameterization and interpolation of irregular data using natural neighbours. *Geophysical Journal International*, *122*, 837–857.

Scheidl, C., Rickenmann, D., & Chiari, M. (2008). The use of airborne LiDAR data for the analysis of debris flow events in Switzerland. *Natural Hazards and Earth System Sciences*, *8*, 1113–1127.

Sibson, R. (1981). A brief description of natural neighbour interpolation (Chapter 2). In V. Barnett. (Ed.), *Interpreting multivariate data* (pp. 21–36). Chichester: John Wiley.

Srinivasan, R., & Engel, B. A. (1991). Effect of slope prediction methods on slope and erosion estimates. *Applied Engineering in Agriculture*, *7*(6), 779–783.

Stoker, J. M., Tyler, D. J., Turnipseed, D. P., Van Wilson, K., Jr., & Oimoen, M. J. (2009). Integrating disparate LiDAR datasets for a regional storm tide inundation analysis of Hurricane Katrina. *Journal of Coastal Research*, 66–72 Special Issue 53 - Coastal Applications of Airborne Lidar [Brock & Purkis]:.

Suddeth, R. J., Mount, J., & Lund, J. R. (2010). Levee decisions and sustainability for the Sacramento–San Joaquin Delta. *San Francisco Estuary and Watershed Science*, *8*(2).

Tarolli, P., Arrowsmith, J. R., & Vivoni, E. R. (2009). Understanding earth surface processes from remotely sensed digital terrain models. *Geomorphology*. doi:10.1016/j.geomorph.2009.07.005.

Tarolli, P., Sofia, G., & Fontana, G. D. (2010). Geomorphic features extraction from high-resolution topography: Landslide crowns and bank erosion. *Natural Hazards*. doi: 10.1007/s11069-010-9695-2.

United Nations International Strategy for Disaster Reductions (NISDR). (2002). Guideline for reducing flood losses. http://www.unisdr.org/publications/v.php?id=558

United States Army Corps of Engineers (USACE). (2000). *Engineering and design — Design and construction of levees (EM 1110-2-1913)*. .

United States Army Corps of Engineers (USACE). (2008). *Geotechnical levee practice standards operating procedures (SOP) Sacramento District*. .

URS Corporation, J. R. Benjamin & Associates (2009). Delta risk management strategy (DRMS) phase 1. Risk analysis report. *Prepared for the California Department of Water Resources*.

United States Society on Dams (USSD) (2009). *Newsletter*, *147*, .

Weiss, J. L., Overpeck, J. T., & Strauss, B. (2011). Implications of recent sea level rise science for low-elevation areas in coastal cities of the conterminous USA. *A letter. Climatic Change*. doi:10.1007/s10584=011-0024-x.

Zhou, Q., & Liu, X. (2004). Analysis of errors of derived slope and aspect related to DEM data properties. *Computers and Geosciences*, *30*(4), 369–378.